analytical chemistry

Subscriber access provided by BRITISH COLUMBIA INST OF TECH

Article

A new type of redox nano-probe: C60-based nanomaterial and its application in electrochemical immunoassay for doping detection

Ruo Yuan

Anal. Chem., **Just Accepted Manuscript** • Publication Date (Web): 30 Dec 2014

Downloaded from http://pubs.acs.org on December 30, 2014

Just Accepted

"Just Accepted" manuscripts have been peer-reviewed and accepted for publication. They are posted online prior to technical editing, formatting for publication and author proofing. The American Chemical Society provides "Just Accepted" as a free service to the research community to expedite the dissemination of scientific material as soon as possible after acceptance. "Just Accepted" manuscripts appear in full in PDF format accompanied by an HTML abstract. "Just Accepted" manuscripts have been fully peer reviewed, but should not be considered the official version of record. They are accessible to all readers and citable by the Digital Object Identifier (DOI®). "Just Accepted" is an optional service offered to authors. Therefore, the "Just Accepted" Web site may not include all articles that will be published in the journal. After a manuscript is technically edited and formatted, it will be removed from the "Just Accepted" Web site and published as an ASAP article. Note that technical editing may introduce minor changes to the manuscript text and/or graphics which could affect content, and all legal disclaimers and ethical guidelines that apply to the journal pertain. ACS cannot be held responsible for errors or consequences arising from the use of information contained in these "Just Accepted" manuscripts.

ACS Publications
High quality. High impact.

Analytical Chemistry is published by the American Chemical Society. 1155 Sixteenth Street N.W., Washington, DC 20036

Published by American Chemical Society. Copyright © American Chemical Society. However, no copyright claim is made to original U.S. Government works, or works produced by employees of any Commonwealth realm Crown government in the course of their duties.

This document is confidential and is proprietary to the American Chemical Society and its authors. Do not copy or disclose without written permission. If you have received this item in error, notify the sender and delete all copies.

A new type of redox nano-probe: C60-based nanomaterial and its application in electrochemical immunoassay for doping detection

Journal:	*Analytical Chemistry*
Manuscript ID:	ac-2014-03406p.R2
Manuscript Type:	Article
Date Submitted by the Author:	29-Dec-2014
Complete List of Authors:	Han, Jing; Southwest University, Zhuo, Ying; Southwest University, Chai, Yaqin; Southwest University, Xiang, Yun; Southwest University, Yuan, Ruo; Southwest University, Education Ministry Key Laboratory on Luminescence and Real-Time Analysis

SCHOLARONE™
Manuscripts

A new type of redox nano-probe: C_{60}-based nanomaterial and its application in electrochemical immunoassay for doping detection

Jing Han, Ying Zhuo*, Ya-Qin Chai, Yun Xiang and Ruo Yuan*

Key Laboratory of Luminescent and Real-Time Analytical Chemistry (Southwest University), Ministry of Education, College of Chemistry and Chemical Engineering, Southwest University, Chongqing 400715, China

* Corresponding authors:

Tel.: +86 23 68252277, fax: +86 23 68253172.

E-mail addresses: yingzhuo@swu.edu.cn (Y. Zhuo), yuanruo@swu.edu.cn (R. Yuan).

ABSTRACT:

Carbon nanomaterials were usually exploited as nanocarriers in electrochemical immunosensor, but rarely acted as redox nano-probes. Herein, our motivation is to adequately utilize the inner redox activity of fullerene (C_{60}) to obtain a new type of redox nano-probe based on a hydrophilic C_{60} nanomaterial. Firstly, C_{60} nanoparticles (C_{60}NPs) were prepared by phase-transfer method and functionalized with amino-terminated polyamidoamine (PAMAM) to obtain the PAMAM decorated C_{60}NPs (PAMAM-C_{60}NPs) which have better hydrophilicity compared to that of unmodified C_{60}NPs and possesses abundant amine groups for further modification. Following that, gold nanoparticles (nano-Au) were absorbed on PAMAM-C_{60}NPs surface, and the resultant Au-PAMAM-C_{60}NPs were employed as a new type of redox nano-probe and nanocarrier to label detection antibodies (Ab_2). Doping control has become the biggest problem facing international sport. Erythropoietin (EPO) as a blood doping agent has been a hotspot in doping control. After sandwich-type immunoreaction between EPO (as a model) and Ab_2-labeled Au-PAMAM-C_{60}NPs, the resultant immunosensor was further incubated with a drop of tetraoctylammonium bromide (TOAB) which acts as booster to arouse the inner redox activity of Au-PAMAM-C_{60}NPs, thus a pair of reversible redox peaks is observed. As a result, the proposed immunosensor shows a wide linear range and a relatively low detection limit for EPO. This strategy paves a new avenue for exploring the redox nano-probe based on carbon nanomaterials in electrochemical biosensor filed.

INTRODUCTION

Doping abuse has worsened considerably over recent years to become the biggest problem facing international sport.[1] Erythropoietin (EPO) is the most important peptide hormone (MW circa 34 KDa) that as a blood doping agent has been a hotspot in doping control area in recent years.[2,3] Therefore, a highly sensitive analytical method for the detection of EPO is strongly desired. As an important research area of analytical chemistry, electrochemical immunoassay has gained considerable interest for its intrinsic advantages such as high sensitivity, low cost and good portability.[4,5] Because most immune proteins are not intrinsically able to act as redox partners in an immunoassay reaction, the effective immobilization of redox molecule is a key step in the construction of sandwich-type immunosensor, which determines the detection limit, linear range and sensitivity.[6] Initially, the most immunoreactions are based on the addition of redox molecules (i.e., potassium hexacyanoferrate, thionine, ferrocene) into testing solution to monitor the current response before and after the specific binding of antibody and antigen.[7] Recently, the label of redox molecule with detection antibodies (Ab_2), especially combined with nanomaterial (carbon nanotubes, graphene) has been mainstream strategy to construct a sandwich-type immunosensor, which avoided the addition of redox molecules to the solution.[8,9] Very recently, nanomaterial itself as redox probe (such as Prussian blue, metallic hexacyanoferrates) has been widely used because of (i) enhancing the amount of immobilized biomolecules as nanocarriers and (ii) avoiding the leakage of redox molecules efficiently.[10-12] Therefore, searching for a new type of nanomaterial-based probe with intrinsic redox

activity, good biocompatibility and chemical stability is still highly desired.

Inspiringly, carbon nanomaterials as nanocarriers, especially carbon nanotubes and graphene have been widely applied in the areas of electrochemical biosensors,[13-16] owing to theirs high electronic conductivity, large specific surface area and good biocompatibility.[17-21] Fullerene (C_{60}), a zero-dimensional carbon, is another rapidly rising star on the horizon of materials science.[22] Importantly, excepting for the above advantages of carbon nanotubes and graphene,[23-25] C_{60} owned its inner redox activity, such as strong electron-accepting capacity and ability to form corresponding anionic species.[26,27] For example, Song et al.[28] and Liu et al.[29] have demonstrated that C_{60} embedded in tetraoctylammonium bromide (TOAB, a cationic surface active agent) organic film for modifying electrode (C_{60}/TOAB/GCE) shows reversible cyclic voltammograms (CVs) due to electrochemical reaction occurs at the oxidation-reduction for generation of C_{60}/C_{60}^{-}, C_{60}^{-}/C_{60}^{2-} and C_{60}^{2-}/C_{60}^{3-}. Wu and co-workers[30] reported that zinc porphyrin-fullerene derivative (ZnP-C_{60}) was entrapped in TOAB-toluene film to modify electrode (ZnP-C_{60}/TOAB/GCE) and reversible electrochemical redox peaks were also observed. Based on the above observations, the possible mechanism of electrochemical behavior for C_{60} in TOAB-toluene film may be that the positively charged cations tetraoctylammonium (TOA^{+}) made the electron cloud of C_{60} is uneven distribution and easy to polarize. After CV scanning, TOA^{+} could act as booster to arouse the inner redox activity of C_{60} and favor the generation of the negatively charged anions of C_{60} (C_{60}^{n-}) in the film. Thus, C_{60} embedded in TOA^{+} organic film, can easily realize electrochemical redox

reactions but the redox activity of C_{60} in aqueous media is inhibited because the water solubility of C_{60} is very poor and the electrochemical behavior of C_{60} in aqueous is unstable and irreversible.[31] To the best of our knowledge, so far, there is no report focusing on using a hydrophilic C_{60}-based nanomaterial as redox probe for the construction of sandwich-type electrochemical immunosensor.

Our motivation in this work was to adequately utilize the inner redox activity of C_{60} to obtain a new type redox nano-probe for the detection of EPO. To prepare a hydrophilic C_{60}-based redox nano-probe, C_{60} nanoparticles (C_{60}NPs) were first prepared by phase-transfer method and functionalized with amino-terminated polyamidoamine (PAMAM) which is a hyper-branched and three-dimensional structure with good structural homogeneity and high density of surface active groups.[32-34] The PAMAM decorated C_{60}NPs product (PAMAM-C_{60}NPs) have better hydrophilicity compared to that of unmodified C_{60}NPs and possesses abundant amine groups on the surface for further modification. After that nano-Au were absorbed on PAMAM-C_{60}NPs surface *via* amino-Au affinity, and the resultant Au-PAMAM-C_{60}NPs were employed as a new redox nano-probe and nanocarrier to label Ab_2. The immunosensing interface was constructed by effective and directional immobilization of capture antibodies (Ab_1) *via* the bridging of protein A (PA)[35] on the Au nanodendrites (AuNDs) decorated glassy carbon electrode (GCE). After sandwich-type immunoreaction between EPO and Ab_2-labeled Au-PAMAM-C_{60}NPs, the resultant immunosensor was incubated with a drop of TOAB for 10 min and detected in 0.1 M PBS. To our surprise, the inner redox activity of C_{60}-based

nanomaterial (Au-PAMAM-C_{60}NPs) was aroused and a pair of reversible redox peaks between -0.45 and 0.3 V in CVs was obtained. Scheme 1 outlines the synthetic process of Au-PAMAM-C_{60}NPs and the fabrication of the immunosensor, which are discussed in detail in the Experimental Section.

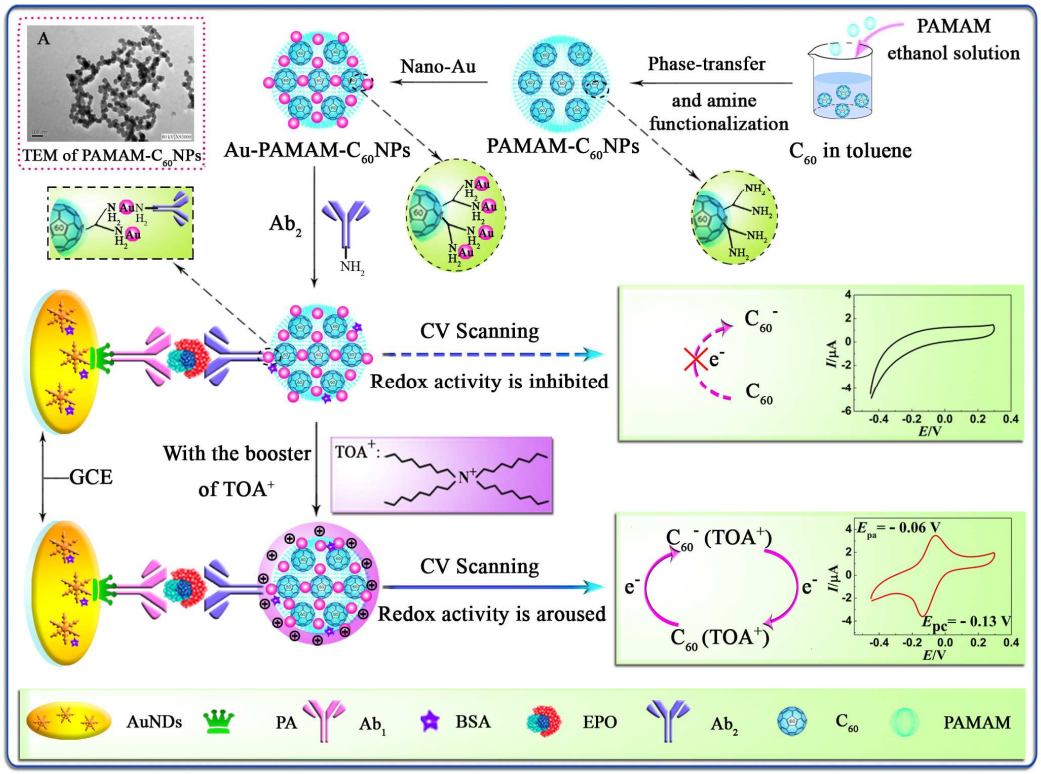

Scheme 1. Schematic Illustration of the Immunosensor Preparation Process and Possible Mechanism of Electrochemical Reaction.

■ EXPERIMENTAL SECTION

Reagents and Material. Erythropoietin (EPO) and EPO antibody (*anti*-EPO, monoclonal antibody) were purchased from SCIPROGEN Bio-pharmaceutical Co. (Shenzhen, China). Fullerene (C_{60}) was provided by Pioneer Nanotechnology Co. (Nanjing, China). Fifth generation (G 5.0) amino-terminated polyamidoamine (PAMAM) dendrimer was supplied by Aldrich (St. Louis, MO, USA). Protein A (PA),

bovine serum albumin (BSA) and gold chloride ($HAuCl_4$) were obtained from Sigma Chemical Co. (St. Louis, MO, USA). Tetraoctylammonium bromide (TOAB, 98%) was purchased from J&K Scientific. Aqueous solutions were prepared using doubly distilled water. Phosphate buffered solution (PBS) as working buffer was employed to investigate the performance of electrodes, which was prepared by mixing Na_2HPO_4, KH_2PO_4 and KCl at a concentration of 0.1 M (pH 7.4).

Apparatus and Measurements. Electrochemical experiments including cyclic voltammetry (CV), differential pulse voltammetry (DPV) and electrochemical impedance spectroscopy (EIS) measurements were recorded with CHI 852C workstation (CH Instruments Co., China). All experiments were performed in a conventional three-electrode system: a modified glassy carbon electrode (GCE, 4 mm diameter) as the working electrode, a saturated calomel electrode (SCE) as the reference electrode and a platinum wire as the auxiliary electrode. The morphology of PAMAM-C_{60}NPs was characterized by transmission electron microscopy (TEM, Hitachi 600, Japan) at an acceleration voltage of 80 kV. Scanning electron micrographs (SEM) were taken with a Hitachi S4800 scanning electron microscope at an acceleration voltage of 20-30 kV. X-ray photoelectron spectroscopy (XPS) analysis was carried out using a VG Scientific ESCALAB 250 spectrometer (Thermoelectricity Instruments, U.S.A.).

Computational Details. All calculations were carried out with Gaussian 09 package using density functional theory (DFT)[36]. The B3LYP approach was used in theoretical calculations[37]. In this work, the geometries of C_{60} and C_{60}^- was optimized

using the 6-31G basis set. Vibrational frequency calculations done at the B3LYP/6-31G level of theory were used to confirm all of the stationary points (NIMAG 0). Electrostatic potential images were made by GuassView 5.0 using the optimized structures of C_{60} and C_{60}^{-}.

Preparation of PAMAM-C_{60}NPs. PAMAM-C_{60}NPs were prepared by phase-transfer method by adding PAMAM ethanol solution into C_{60} toluene solution. In a typical experiment, 1 mg amino-terminated PAMAM was first dissolved in 1 mL aqueous solution, and then 4 mL ethanol was added. Next, the PAMAM mixture solution mentioned above was added to 1 mL C_{60} toluene (1.5 mM) under continuous stirring to obtain abundant -NH_2 groups on the surface of C_{60}NPs. After the reaction for 36 h, the solution was centrifuged and washed respectively with ethanol and doubly distilled water for three times. And then it was dispersed in 2 mL of 0.1 M PBS (pH 7.4). The obtained PAMAM-C_{60}NPs was characterized by TEM (Scheme 1A). It can be seen that a lot of C_{60}NPs have been adsorbed on PAMAM polymerization fiber to form PAMAM-C_{60}NPs, indicating the successful preparation of PAMAM decorated C_{60}NPs.

Preparation of Au-PAMAM-C_{60}NPs. First, gold nanoparticles (nano-Au) were prepared according to the literature.[38] Later, nano-Au solution was added into the above PAMAM-C_{60}NPs solution (1 mL), and the mixture was stirred at 4 °C for 8 h. Then the product of Au-PAMAM-C_{60}NPs was obtained *via* amino-Au affinity. Afterwards, the mixture was centrifuged (8,000 rpm) for 15 min, the upper solution was removed, and the lower product was washed several times with doubly distilled

water.

Preparation of Au-PAMAM-C_{60}NPs Labeled Ab_2. 100 μL Ab_2 was slowly added into 1 mL Au-PAMAM-C_{60}NPs solution under softly stirring and incubated for 8 h at 4 °C *via* amino-Au affinity between nano-Au of Au-PAMAM-C_{60}NPs and -NH_2 of Ab_2. The obtained Ab_2 bioconjugate (Ab_2-labeled Au-PAMAM-C_{60}NPs) was collected by centrifugation (8,000 rpm) for 20 min to discard excess reagents and finally dispersed in 1 mL PBS and stored at 4 °C for further usage.

Fabrication of the Sensing Interface. To obtain a mirror-like surface, a glassy carbon electrode (GCE, with diameter of 4 mm) was sequentially polished with 0.3 and 0.05 μm alumina slurries, followed by ultrasonic treatment in ethanol and doubly distilled water. The GCE was then allowed to dry at room temperature (RT). In order to obtain a large conductive surface area, a thin layer of Au nanodendrites (AuNDs) was electrochemically deposited onto the pretreated GCE under constant potential electrolysis of 0.0 V for 600 s in the electrolyte containing 2.5 mM $HAuCl_4$, 0.5 M H_2SO_4 and 150 mM EDA according to the literature.[39] Afterwards, the AuNDs/GCE was immersed into 0.2 mg mL^{-1} PA solution and incubated for 6 h for directional and highly efficient immobilization of antibodies. Following that, the prepared PA/AuNDs/GCE was incubated with 0.5 mL of capture EPO antibodies (abbreviated as Ab_1) at 4 °C for 12 h. Finally, the resultant immunosensor was incubated with 20 μL of 1% BSA solution for 0.5 h to block the non-specific binding sites to obtain BSA/Ab_1/PA/AuNDs/GCE.

Measurement Procedure. The measurement was based on the typical procedure of sandwich-type immunoreactions. Before measurement, the as-prepared immunosensor was incubated with various concentrations of 20 μL EPO samples for 1 h at 37 ºC. Subsequently, the immunosensor was further incubated with 20 μL of the prepared Ab_2 bioconjugates (Ab_2/Au-PAMAM-C_{60}NPs) at 37 ºC for 1 h. After each step, the electrode was washed by using PBS to remove the physically absorbed species. Lastly, the resultant immunosensor was incubated with a drop of TOAB toluene (10 mM) for 10 min, which acts as booster to arouse the inner redox activity of Au-PAMAM-C_{60}NPs. Finally, the obtained immunosensor was detected in 0.1 M PBS (pH 7.4) at RT.

■ RESULTS AND DISCUSSION

The Stepwise Immunosensor Fabrication by SEM Characterization. The stepwise immunosensor fabrication processes were monitored by SEM. Fig. 1A showed that AuNDs were straightforwardly electrodeposited on the conductive glass, we can found that well-defined dendritic structures are arranged along a backbone with symmetrical side branches. Upon the immobilization of PA on the AuNDs surface, an image with a blurry surface was observed (Fig. 1B), which is distinct from that of Fig. 1A, indicating the successful bonding of the PA on the surface. Subsequently, with loading of Ab_1 onto PA/AuNDs film, a dense protein layer was obtained (Fig. 1C), suggesting that the Ab_1 was successfully introduced *via* the bridging of PA.

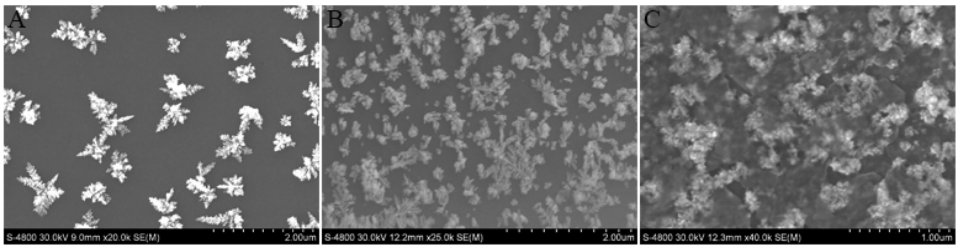

Fig. 1 SEM images of (A) AuNDs, (B) PA/AuNDs and (C) Ab_1/PA/AuNDs.

XPS Characterization of Au-PAMAM-C_{60}NPs. To prove the successful synthesis of Au-PAMAM-C_{60}NPs, XPS characterization was used for elemental analysis. As expected, characteristic peaks for C1s, N1s, O1s and Au4f regions could be clearly observed in the full region of Au-PAMAM-C_{60}NPs spectrum (Fig. 2A). The peaks at 284.7 eV, 399.8 eV and 532.4 eV could be assigned to C1s, N1s and O1s, respectively (Fig. 2B, 2C and 2D). Fig. 2E represents the XPS signature of the Au4f doublet (84.0 eV and 87.7 eV for the $4f_{7/2}$ and $4f_{5/2}$, respectively) for the resulting metallic Au^0. Based on the above elemental analysis, we could confirm that the Au-PAMAM-C_{60}NPs were successfully prepared.

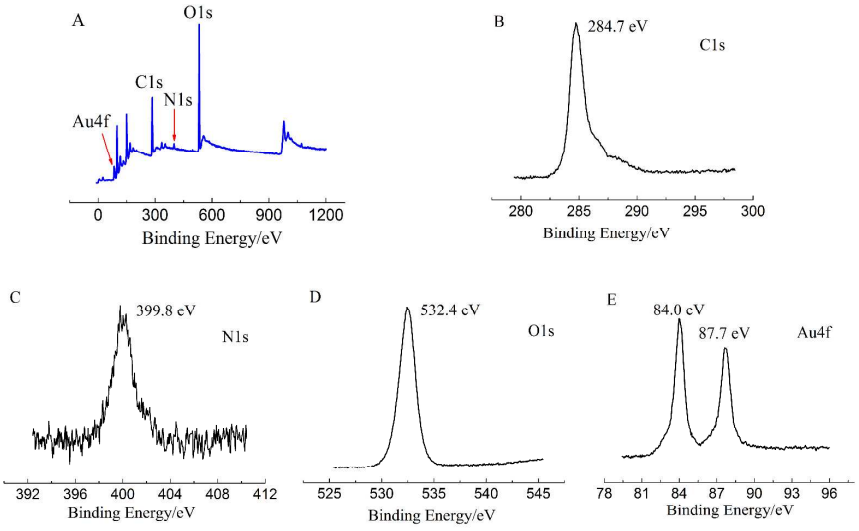

Fig. 2 XPS analysis for (A) the full region of XPS for Au-PAMAM-C_{60}NPs, (B) C1s region, (C) N1s region, (D) O1s region and (E) Au4f region.

Electrochemical Behaviors of the Electrochemical Immunosensor. To confirm the fabrication process of the immunosensor, CV and EIS measurements were used to characterize the stepwise assembled processes in 0.1 M PBS (pH 7.4) containing 5 mM $[Fe(CN)_6]^{4-/3-}$. As shown in Fig. 3A, curve *a* exhibited a pair of reversible redox peaks, corresponding to the reversible redox reaction of ferricyanide ions on the bare GCE. When AuNDs were straightforwardly electrodeposited on the GCE, the peak current was obviously increased (Fig. 3A, curve *b*), implying that AuNDs brought excellent conductivity and large surface area to promote the electron transfer. However, when PA was immobilized onto the AuNDs/GCE (Fig. 3A, curve *c*), the CV response was decreased significantly, as the PA may act as the electron transfer blocking layer and hinder the diffusion of ferricyanide toward the electrode surface. Subsequently, when Ab_1 was introduced *via* the bridging of PA, an obvious decrease in redox current was observed (Fig. 3A, curve *d*). Furthermore, the CV response decreased after the resultant electrode blocking with 1% BSA solution (Fig. 3A, curve *e*). Finally, when the resulted immunosensor was incubated with 40 mIU mL^{-1} EPO, the CV response was decreased again (Fig. 3A, curve *f*). Such decreases can be basically attributed to the fact that the Ab_1, BSA and EPO protein layers on the electrode would retard the electron transfer.

EIS of different modified electrodes was shown in Fig. 3B. In the Nyquist plots, the semicircle diameter of EIS is equal to R_{et}. The bare GCE showed a small semicircle (Fig. 3B, curve *a*), indicating a low electron-transfer resistance. When AuNDs were electrodeposited on the electrode surface, the Nyquist diagram is

approximately a straight line (Fig. 3B, curve *b*), suggesting the excellent conductive properties of porous AuNDs film. After incubating with PA solution, the resistance was increased (Fig. 3B, curve *c*) because the PA as an electron transfer blocking layer hindered the diffusion of ferricyanide to the electrode surface. Subsequently, when Ab_1, BSA and EPO were successively immobilized on the electrode surface, the resistance increased orderly (Fig. 3B, curves *d*, *e* and *f*). The experiment results clearly demonstrated that EIS characterization is in accordance with CV measurement.

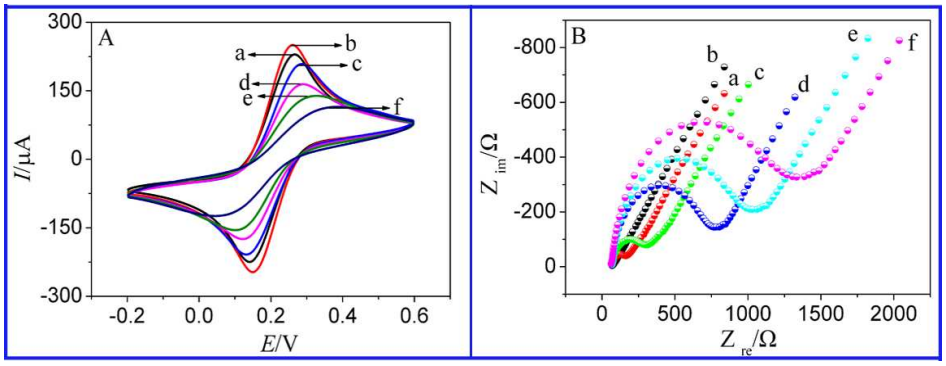

Fig. 3 CVs (A) and EIS (B) of different modified electrodes in pH 7.4 PBS containing 5 mM $[Fe(CN)_6]^{4-/3-}$ as redox probe: (a) bare GCE, (b) AuNDs/GCE, (c) PA/AuNDs/GCE, (d) Ab_1/PA/AuNDs/GCE, (e) BSA/Ab_1/PA/AuNDs/GCE, (f) after incubation with 40 mIU mL^{-1} EPO.

In order to investigate the role of Au-PAMAM-C_{60}NPs in TOAB system, CVs of different modified electrodes was studied in Fig. 4A. Curve *a* showed CVs recorded at EPO/BSA/Ab_1/PA/AuNDs/GCE and then successively incubated with Ab_2 bioconjugate (Ab_2-labeled Au-PAMAM-C_{60}NPs) and TOAB. As expected, the proposed immunosensor was detected in PBS (pH 7.4) and showed a pair of reversible redox peaks. The anodic and cathodic peak potentials are E_{pa} = - 0.06 V and

E_{pc} = - 0.14 V (*vs.* SCE), respectively, and the peak-to-peak separation is 80 mV, which is in agreement with the work of Song et al.[28] Furthermore, the control experiments were also done. In order to demonstrate that the inner redox activity of Au-PAMAM-C_{60}NPs are aroused by TOA^+, the EPO/BSA/Ab_1/PA/AuNDs/GCE only incubated with Ab_2 bioconjugate was investigated and no redox peaks were observed in the potential range (Fig. 4A, curve *b*). To further verify whether the TOA^+ itself has redox activity, the EPO/BSA/Ab_1/PA/AuNDs/GCE only incubated with TOAB was also investigated and no redox peaks were found (Fig. 4A, curve *c*). This comparison clearly demonstrated that TOA^+ acts as booster to arouse the inner redox activity of Au-PAMAM-C_{60}NPs, thus a pair of reversible redox peaks was observed.

To further explore the reversibility of electron transfer process, the CVs of the prepared immunosensor at different scan rates were detected in PBS (pH 7.4), as shown in Fig. 4B. It can be found that both the anodic and cathodic peak currents are proportional to the square root of scan rates in the range of 20-700 mV s^{-1} and exhibit a linear relationship, suggesting that the electrochemical reaction at the prepared electrode is a diffusion-controlled electrochemical process.

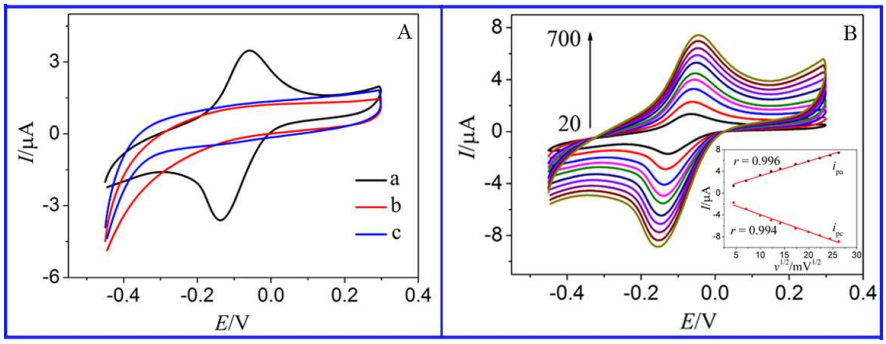

Fig. 4 A: CVs of different modified electrodes in pH 7.4 PBS after incubation with 40 mIU mL^{-1} EPO, and then successive incubation with Ab_2 bioconjugate and TOAB (a); incubation with Ab_2

bioconjugate without TOAB (b); incubation with TOAB in the absence of Ab_2 bioconjugate (c). B: CVs of the proposed immunosensor at different scan rates (from inner to outer): 20, 50, 100, 150, 200, 300, 400, 500, 600 and 700 mV s^{-1} in pH 7.4 PBS. Insert: plots of the redox peak currents *vs* the square root of scan rate. All potentials are given versus SCE.

Possible Mechanism of Electrochemical Reaction. As supported by the experimental results in Fig. 4, the possible electrochemical mechanism was shown in Scheme 2A. When TOA^+ is not existed, electron cloud of C_{60} is uniform distribution and difficult to polarize, so C_{60} is difficult to reduce and no redox peaks are observed in the potential range. Inspiringly, when TOA^+ is existed, the numerous positively charged TOA^+ are absorbed on C_{60} surface, which made the electron cloud of C_{60} is uneven distribution and easy to polarize. After CV scanning from -0.45 to 0.3 V, TOA^+ could act as booster to arouse the inner redox activity of C_{60} and favor the generation of the negatively charged anions of C_{60} (C_{60}^-) in the film, thus a pair of reversible redox peaks is observed. Moreover, according to the computational model, we have calculated the electrostatic potential (ESP) on van der Waals (vdW) surface and the highest occupied molecular-orbital (HOMO) of C_{60} and C_{60}^-. ESP on vdW surface represents C_{60} and C_{60}^-, respectively, as shown in Scheme 2B. It can be seen that the ESP has changed from neutral ESP (Scheme 2B-a) to negative ESP (Scheme 2B-b), indicating the generation of C_{60}^-. Molecular orbital is further applied to investigate the electronic properties of C_{60} and C_{60}^- and displayed in Scheme 2C. When C_{60} is polarized to C_{60}^-, the electronic configuration of C_{60} in HOMO has changed and owns negative charge. On the basis of the computational studies, we can

conclude that our presumed electrochemical mechanism is reasonable.

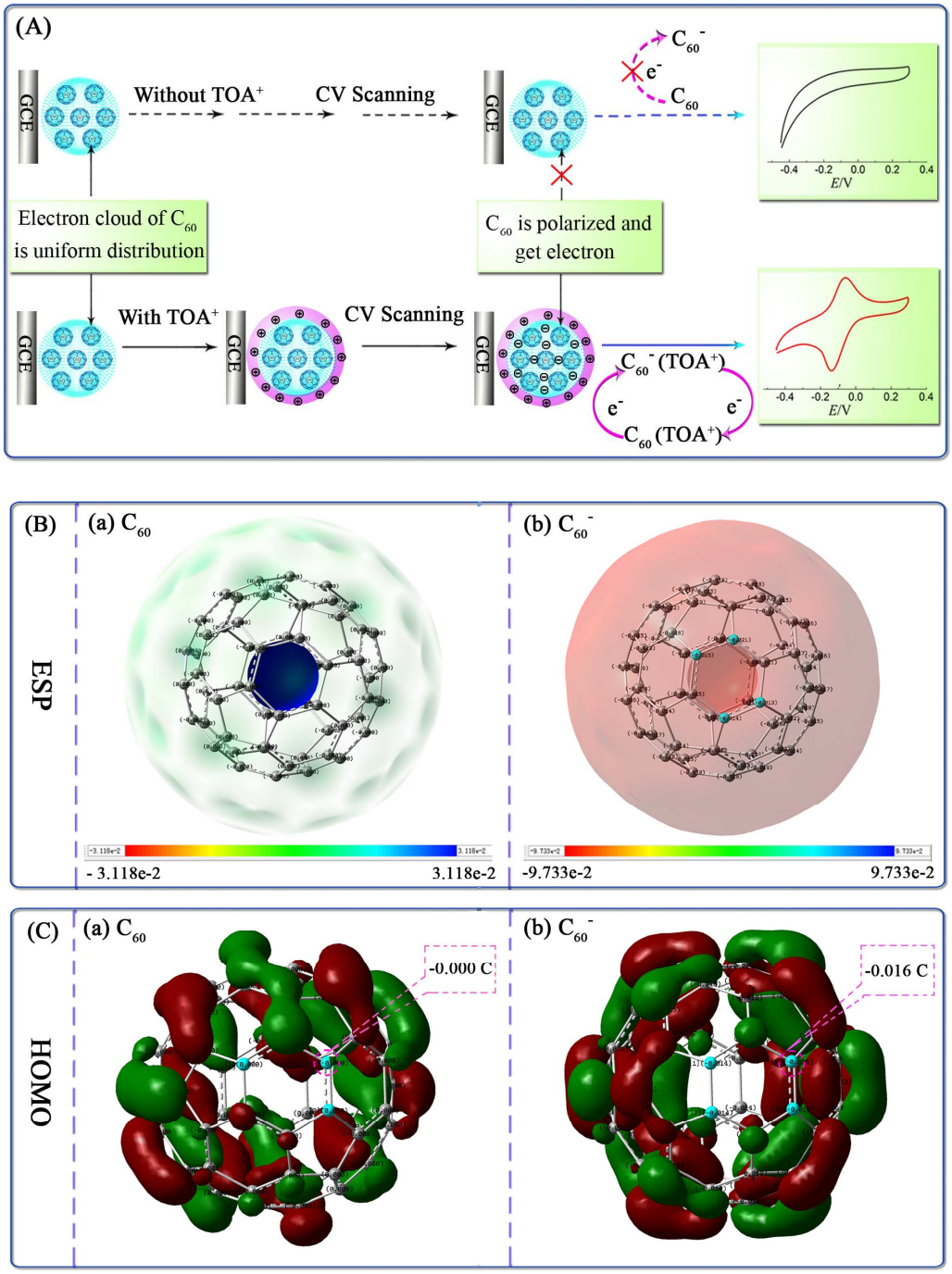

Scheme 2. (A) Possible mechanism of electrochemical reaction. (B) ESP mapped molecular vdW surface of C_{60} (a) and C_{60}^{-} (b). The minima and maxima of ESP are labeled by red and blue, respectively. (C) HOMO of C_{60} (a) and C_{60}^{-} (b).

Analytical Performance of the Immunosensor. To investigate the sensitivity and quantitative range of the proposed immunoassay, the developed immunosensors were employed to detect the different concentrations of EPO standard solutions with DPV technique in 0.1 M PBS (pH 7.4). It can be seen (Fig. 5A) that the DPV responses of the immunosensor increased with the increasing concentrations of EPO. In Fig. 5B, the calibration plot shows a good linear relationship between the currents and the logarithmic values of EPO concentrations ranging from 0.01 to 80 mIU mL^{-1} with a correlation coefficient of 0.996. The regression equation is $I = 0.681 \lg c_{EPO} + 2.113$ with a detection limit of 0.0027 mIU mL^{-1} at 3σ (where σ is the standard deviation of the blank signals, $n = 20$). The result indicated that the proposed immunosensor could be used to detect EPO quantitatively.

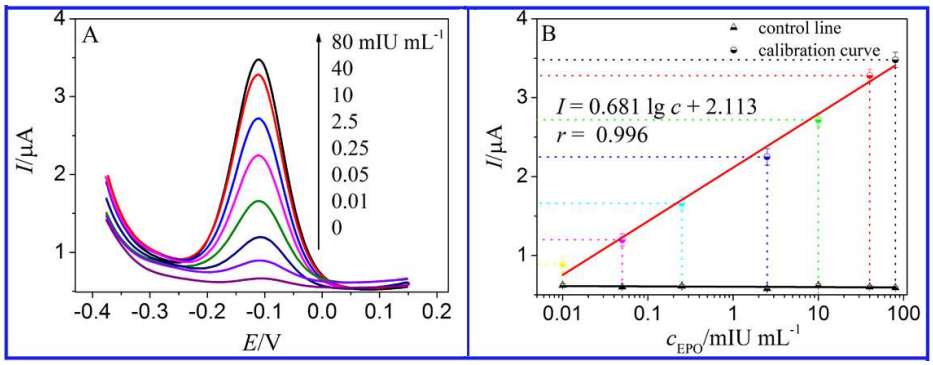

Fig. 5: DPV responses (A) and calibration curves (B) of the proposed immunosensor after incubation with different concentrations of EPO standard solutions.

Specificity, Stability and Reproducibility of the Immunosensor. Specificity is an important factor of the antigen-antibody binding. The potential interfering substances in serum, such as, immunoglobulin G (IgG), human serum albumin (HSA) and platelet-derived growth factor (PDGF) were used to evaluate the specificity of the

proposed immunosensor. As seen from Fig. 6A, no apparent change in the current was obtained compared with that of the blank test. Nevertheless, a dramatic increase was found in the presence of target EPO. Even when IgG, HSA and PDGF were coexisted with EPO, the DPV response was almost the same with that of EPO alone. These results indicated the high specificity of the proposed assay for EPO detection. The long-term storage stability was performed by storing the prepared immunosensor at 4 ºC and measuring every one week. As shown in Fig. 6B, no obvious change was found during the first week and the response changed less than 8.2% of the original current. After storing for two weeks, it maintained 86.3% of the initial response, implying that our proposed immunosensor is of acceptable stability. The reproducibility of the immunosensor was studied by intra- and inter-assay coefficients of variation (DPV) according to the following methods: the intra-assay was estimated by analyzing EPO level (40 mIU mL^{-1}) for five times using the same prepared immunosensor, and a relative standard deviation (RSD) of 4.0% was acquired. The inter-assay was evaluated by analyzing the EPO using five equally immunosensors under the same conditions, where all electrodes showed approximate electrochemical responses and a RSD of 6.2% were obtained. The experiment results implied that the fabricated immunosensor hold potentials for quantitative assay of EPO with desirable reproducibility.

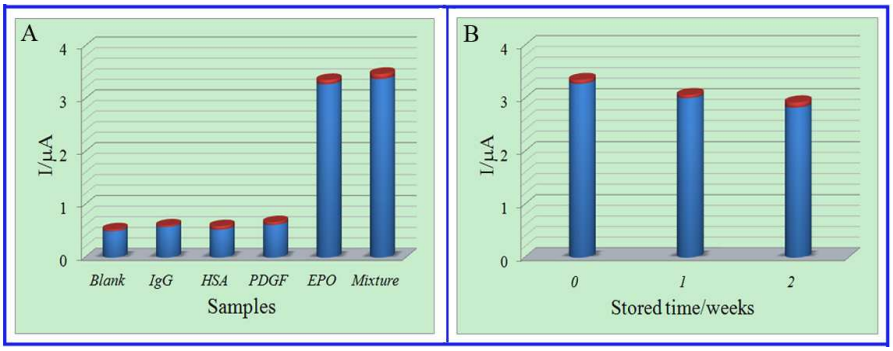

Fig. 6 A: The selectivity of the immunosensor: IgG (80 nM), HSA (80 nM), PDGF (80 nM), EPO (40 mIU mL^{-1}) and the mixture. B: The stability of immunosensor for 0 week, 1 week and 2 weeks, respectively (error bars: SD, n = 3).

Application. To test the applicability of the proposed electrochemical immunosensor for EPO analysis in real samples, a series of human serum samples from the Ninth People's Hospital (Chongqing, China) were monitored by the developed strategy. In parallel, the same sampled were also detected with commercially enzyme-linked immunosorbent assay (ELISA) method. As can be seen from Table 1, the relative deviations between two methods are in the range of -8.75−9.76, which clearly demonstrated the potentiality of the proposed immunosensor for the analytical application in real biological samples.

Table 1. Comparison of serum EPO levels determined using two methods.

Sample No.	DPV method/mIU mL^{-1}	ELISA/mIU mL^{-1}	Relative deviation/%
1	0.024	0.025	-4.00
2	1.219	1.250	-2.48
3	3.378	3.200	5.56
4	5.340	5.000	6.80
5	10.95	12.00	-8.75
6	13.72	12.50	9.76

■ CONCLUSIONS

In short, the hydrophilic C_{60}-based nanomaterial (Au-PAMAM-C_{60}NPs) was first synthesized and employed as a new type of redox nano-probe to construct a sandwich-type immunosensor for EPO detection. It is worth noticing that the proposed immunosensor had good sensitivity, stability and reproducibility, showing potential applications in doping control as well as bioanalysis. More importantly, this strategy may pave a new avenue for exploring the carbon-based materials as redox nano-probe to fabricate various electrochemical immunosensors, promising for the routine biosensing application.

■ AUTHOR INFORMATION

* Corresponding authors:

Tel.: +86 23 68252277, fax: +86 23 68253172.

E-mail addresses: yingzhuo@swu.edu.cn (Y. Zhuo), yuanruo@swu.edu.cn (R. Yuan).

Notes

The authors declare no competing financial interest.

■ ACKNOWLEDGMENTS

This research was supported by the NNSF of China (21275119, 21105081 and 51473136), Research Fund for the Doctoral Program of Higher Education (RFDP) (20110182120010), Ministry of Education of China (Project 708073) and Natural Science Foundation Project of Chongqing City (CSTC-2010BB4121, CSTC-2011BA7003), the Fundamental Research Funds for the Central Universities

(XDJK2013008, XDJK2013A027 and XDJK2014A012), China. Great thanks to Prof. Ming Li of Southwestern University for helping with the theoretical data analysis.

■ REFERENCES

(1) Citartana, M.; Gopinath, S. C. B.; Chen, Y.; Lakshmipriya, T.; Tang, T. H. *Biosens. Bioelectron.* **2015**, *63*, 86–98.

(2) Kai, S.; Tanaka, T.; Matsuyama, T.; Suzuki, K.; Hirota, K. *Eur. J. Pharmacol.* **2014**, *732*, 43–49.

(3) Lasne, F.; Ceaurriz, J. D. *Nature*, **2000**, *405*, 635–637.

(4) Li, X. M.; Yang, X. Y.; Zhang, S. S. *TrAC, Trends Anal. Chem.* **2008**, *27*, 543–553.

(5) Tang, J.; Tang, D. P.; Niessner, R.; Chen, G. N.; Knopp, D. *Anal. Chem.* **2011**, *83*, 5407–5414.

(6) Wang, L.; Zhang, Q. Y.; Chen, S. L.; Xu, F. G.; Chen, S. H.; Jia, J. B.; Tan, H. L.; Hou, H. Q.; Song, Y. H. *Anal. Chem.* **2014**, *86*, 1414−1421.

(7) Ho, J. A. A.; Chang, H. C.; Shih, N. Y.; Wu, L. C.; Chang, Y. F.; Chen, C. C.; Chou, C. *Anal. Chem.* **2010**, *82*, 5944–5950.

(8) Loo, A. H.; Bonanni, A.; Ambrosi, A.; Poh, H. L.; Pumera, M. *Nanoscale* **2012**, *4*, 921–925.

(9) Jia, X. L.; Chen, X.; Han, J. M.; Ma, J.; Ma, Z. F. *Biosens. Bioelectron.* **2014**, *53*, 65–70.

(10) Liu, N.; Ma, Z. F. *Biosens. Bioelectron.* **2014**, *51*, 184–190.

(11) Lai, G. S.; Yan, F.; Ju, H. X. *Anal. Chem*. **2009,** *81*, 9730–9736.

(12) Han, J.; Zhuo, Y.; Chai, Y. Q.; Yuan, R.; Zhang, W.; Zhu, Q. *Anal. Chim. Acta* **2012**, *746*, 70–76.

(13) Kong, F. Y.; Xu, B. Y.; Du, Y.; Xu, J. J.; Chen, H. Y. *Chem. Commun*. **2013**, *49*, 1052–1054.

(14) Akter, R.; Rahman, M. A.; Rhee C. K. *Anal. Chem*. **2012**, *84*, 6407−6415.

(15) Lai, G. S.; Wu, J.; Ju , H. X.; Yan, F. *Adv. Funct. Mater.* **2011**, *21*, 2938–2943.

(16) Du, D.; Wang, L. M.; Shao, Y. Y.; Wang, J.; Engelhard, M. H.; Lin Y. H. *Anal. Chem*. **2011**, *83*, 746–752.

(17) Li, F.; Yu, Y. Q.; Li, Q.; Zhou, M.; Cui, H. *Anal. Chem*. **2014**, *86*, 1608–1613.

(18) Liu, H. Y.; Xu, S. M.; He, Z. M.; Deng, A. P.; Zhu, J. J. *Anal. Chem*. **2013**, *85*, 3385−3392.

(19) Liu, G. D.; Shen, H.; Mao, J. N.; Zhang, L. M.; Jiang, Z.; Sun, T.; Lan, Q.; Zhang, Z. J. *ACS Appl. Mater. Interfaces* **2013**, *5*, 6909−6914.

(20) Chen, D.; Feng, H. B.; Li, J. H. *Chem. Rev*. **2012**, *112*, 6027−6053.

(21) Zeng, Q.; Cheng, J. S.; Tang, L. H.; Liu, X. F.; Liu, Y. Z.; Li, J. H.; Jiang J. H. *Adv. Funct. Mater.* **2010**, *20*, 3366–3372.

(22) Feng, M.; Zhao, J.; Petek, H. *Science* **2008**, *320*, 359–362.

(23) Han, J.; Zhuo, Y.; Chai, Y. Q.; Yuan, R.; Xiang, Y.; Zhu, Q.; Liao, N. *Biosens. Bioelectron.* **2013**, *46*, 74–79.

(24) Zhong, X,; Yuan, R.; Chai, Y. Q. *Chem. Commun.* **2012**, *48*, 597–599.

(25) Wang, H. J.; Bai, L. J.; Chai, Y. Q.; Yuan, R. *Small* **2014**, *10*, 1857–1865.

(26) Zhou, M.; Guo, J.; Guo, L. P.; Bai, J. *Anal. Chem.* **2008**, *80*, 4642−4650.

(27) Stuart, E. J. E.; Tschulik, K.; Batchelor-McAuley, C.; Compton, R. G. *ACS Nano* **2014**, *8*, 7648–7654.

(28) Song, F. Y.; Echegoyen, L. *J. Phys. Chem. B* **2003**, *107*, 5844−5850.

(29) Liu, W.; Gao, X. *Electrochem. Commun.* **2008**, *10*, 1377–1380.

(30) Wu, H.; Fan, S. H.; Jin, X. Y.; Zhang, H.; Chen, H.; Dai, Z.; Zou, X. Y. *Anal. Chem.* **2014**, *86*, 6285–6290.

(31) Lopez, A. L.; Mateo-Alonso, A.; Prato, M. *J. Mater. Chem.* **2011**, *21*, 1305–1318.

(32) Jeong, B. J.; Akter, R.; Han, O. H.; Rhee, C. K.; Rahman, M. A. *Anal. Chem.* **2013**, *85*, 1784−1791.

(33) Liu, X.H.; Ma, D. M.; Tang, H.; Tan, L.; Xie, Q. J.; Zhang, Y. Y.; Ma, M.; Yao, S. Z. *ACS Appl. Mater. Interfaces* **2014**, *6*, 8173−8183.

(34) Astruc, D.; Boisselier, E.; Ornelas, C. *Chem. Rev*. **2010**, *110*, 1857−1959.

(35) Zhao, W. W.; Shan, S.; Ma, Z. Y.; Wan, L. N.; Xu, J. J.; Chen, H. Y. *Anal. Chem.* **2013**, *85*, 11686–11690.

(36) Frisch, M. J.; Trucks, G. W.; Schlegel, H. B., et al. Gaussian 09, revision A. 02; Gaussian, Inc.: Wallingford, CT, 2009.

(37) Yang, L.; Ling, Y.; Zhang, Y.*J. Am. Chem. Soc*. **2011**, *133*, 13814−13817.

(38) Schwartzberg, A. M.; Olson, T. Y.; Talley, C. E.; Zhang, J. Z. *J. Phys. Chem. B* **2006**, *110*, 19935−19944.

(39) Feng, J. J.; Li, A. Q.; Lei, Z.; Wang, A. J. *ACS Appl. Mater. Interfaces* **2012**, *4*, 2570–2576.

For TOC only

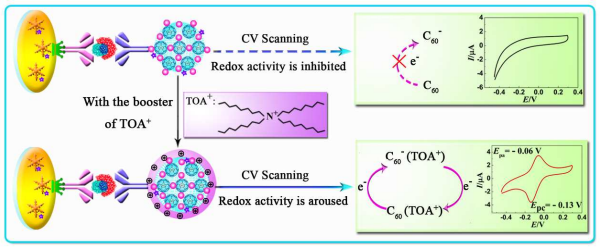
CV Scanning
Redox activity is inhibited
With the booster
of TOA+
CV Scanning
Redox activity is aroused